

NASA reports

30p

CAT. 23

BOUNDARY LAYER NOISE RESPONSE SIMULATION

WITH A SOUND FIELD

NASA CR 56074

Richard H. Lyon

Bolt Beranek and Newman Inc.  
Cambridge, Massachusetts

April 1964

To be presented at the  
Second  
International Conference  
on  
Acoustical Fatigue

Paper B-5

GPO PRICE \$ \_\_\_\_\_

OTS PRICE(S) \$ \_\_\_\_\_

Hard copy (HC) \$ 2.00

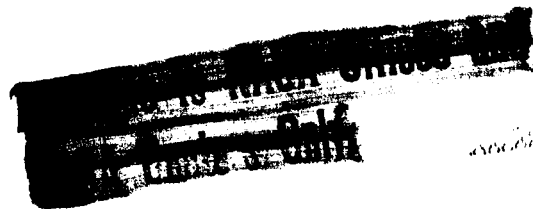
Microfiche (MF) \$ 0.50

Facility Form 602

(THRU)	(CODE)	(CATEGORY)
1	23	
(ACCESSION NUMBER)	(PAGES)	(NASA CR OR TMX OR AD NUMBER)
N65 15362	30	CR 56074

## TABLE OF CONTENTS

I.	Introduction . . . . .	1
II.	Response of a simple structure to boundary layer noise . . . . .	3
	1. Low speed convection, $U_c \ll c_B$ . . . . .	3
	2. High speed convections, $U_c > c_B$ . . . . .	5
III.	Response of a supported panel to a sound field . . . . .	9
IV.	Equivalence between turbulent and acoustic excitation . . . . .	12
V.	Spectral simulation with a sound field . . . . .	16
VI.	Acknowledgement . . . . .	18
	References . . . . .	19
	Figures	



## I. Introduction

The take-off and launch phases of aircraft and spacecraft produce very severe acoustic environments for the structure, personnel, and equipments. The need for accurate data on the response and fatigue (or malfunction) of these vehicles has led engineers to the construction of elaborate and costly facilities for the simulation of intense acoustic environments. A well known example is the Sonic Fatigue Facility being completed at Wright Field. Another is the intense low frequency acoustic facility at Langley Field.

In the flight regimes of these vehicles represented by large dynamic head  $q$ , excitation by the turbulent boundary layer can become a very important source of skin vibration and interior noise. Some of the Mercury shots for example showed that the noise and vibration levels during the "max  $q$ " period significantly exceed those experienced during the launch phase.<sup>1/</sup> The magnitude and importance of these environmental loads naturally leads one to inquire whether an acoustic facility can be used to simulate these loads or their effects.

The simulation of turbulent boundary layer loads would ideally mean the reproduction of the distribution of acoustic pressures over the vehicle with correlation and convection properties very close to those of the turbulence. In a sound

field, the speed of propagation, the wavelength, and the frequency are related. This is not the case for the turbulent field where a particular wavelength component may have a whole distribution of frequencies and/or convection speeds.<sup>2/</sup>

If one is concerned primarily with vibratory response, then it is the turbulent energy at wavelengths near the free bending wavelength in the panel which account for most of the excitation.<sup>3/</sup> Even if one restricts the simulation to this small group of wavenumbers near the bending wavenumber, the simulation of loads is still not possible since the acoustic frequencies at these wavelengths would generally be higher than the frequencies in the panel.

In spite of these difficulties, however, it does appear that one has a chance to simulate the resonant response of a turbulent boundary layer by the response to a sound field, which is, after all, the important thing as far as vibration, malfunction, and fatigue are concerned. The corresponding sound transmission through the structure might not in fact be properly simulated since it depends a good deal on the non-resonant or forced motion of the structure.

## II. Response of a simple structure to boundary layer noise

The vibratory response of the modes of a simply supported thin panel to convected turbulence was computed by Dyer.<sup>4/</sup> He distinguished three primary categories of modal behavior; when the trace wavespeed in the panel projected along the direction of convection is

- a. less than the convection speed, the modes are called hydrodynamically slow (HS)
- b. equal to the convection speed, hydrodynamically coincident (HC)
- c. greater than the convection speed, hydrodynamically fast (HF).

These regimes are readily displayed in wavenumber space as shown in Fig. 1. The trace wavespeed in the direction of convection is  $c_B/\cos\phi$  and the locus of modes for which  $c_B/\cos\phi = U_c$  is the "HC mode" semicircle of radius  $U_c/2kc_g$ . The HS modes fall with this circle, the HF modes without.

### 1. Low speed convection, $U_c \ll c_B$

Dyer's model of the pressure correlation pattern was

$$\overline{p(x_1, t)p(x', t')} = p_h^2 A_t \delta[(x_1 - x'_1 - U_c(t - t'))] \delta(x_3 - x'_3) e^{-|t - t'|/\theta} \quad (1)$$

where  $p_h$  is the turbulent rms pressure,  $U_c$  is the convection speed, and  $A_t$  is a correlation area. When  $U_c \ll c_B$ , the HC locus in Fig. 1 collapses to the origin and the response is composed entirely of HF modes. By grouping the modes in frequency bands, one can compute the spectral density of panel velocity. The result is 5/

$$\mathcal{U}(\omega) = p_h^2 G_\omega A_t \mathcal{P}_T(\omega) / \omega \eta \rho_s \quad (2)$$

where  $G_\omega = (8\rho_s k c_\ell)^{-1}$  is the mechanical point input conductance of an infinite flat plate. In Eq. (1) the moving axis frequency spectrum is

$$\mathcal{P}_T(\omega) = \frac{\theta}{\pi} (1 + \omega^2 \theta^2)^{-1} \quad , \quad (3)$$

although this precise form is not required for the validity of (2). The form of  $\mathcal{P}_T(\omega)$  is shown in Fig. 2, there generally being fairly uniform energy content up to a frequency  $\omega = 1/\theta$ , beyond which the energy diminishes rapidly. The loss factor for the panel is  $\eta$  and  $\rho_s$  is the surface mass density.

The "correlation area"  $A_t$  is determined by the strength of the wavenumber spectrum at the free bending wavenumber for the plate. It is 6/

$$A_t = 4\pi^2 \left\langle \rho_x(k = k_p, \phi) \right\rangle_\phi \quad (4)$$

where  $\rho_x(k)$  is normalized to have unit area. The form of  $A_t$  for low speed (incompressible) turbulence is given in Fig. 3. <sup>7</sup> The excitation is seen to be most effective in the range where the bending wavelength is the reciprocal of the displacement thickness, and drops off above and below this value. We note from (2) that the frequency spectrum  $\rho_r(\omega)$  is directly reflected in the response spectral density.

## 2. High speed convections, $U_c > c_B$

When the convection speed exceeds the trace wavespeed, which is the situation depicted in Fig. 1, one may again apply Dyer's results. In this instance, however, it is useful to compute the power input to an infinite panel since the calculations are simpler to perform and lead to the same results after one averages over groups of modes.

For the infinite panel, one begins with the equation of motion

$$\kappa^2 c_\ell^2 \nabla^4 y + \frac{\partial^2 y}{\partial t^2} + \omega \eta \frac{\partial y}{\partial t} = \frac{p}{\rho_s} \quad (5)$$

and expresses the displacement  $y$  and pressure  $p$  as Fourier integrals in time and space. The power input per unit area of the panel becomes <sup>8</sup>/

$$\Pi = - i p_h^2 \int \omega d\omega \int d\tilde{k} \frac{\mathcal{P}(\tilde{k}, \omega')}{\rho_p h c_\ell^2 [k^4 - k_p^4 (1 + i\eta)]} \quad (6)$$

where  $\mathcal{P}(\tilde{k}, \omega')$  is the spectral density of the turbulent pressure field in a frame moving at the convections speed. The frequency variable is  $\omega' = \omega - k_1 U_c$  where  $\omega$  is the response frequency and  $k_1$  is the component of wavenumber in the direction of convection.

The spectrum  $\mathcal{P}$  is the transform of the correlation function  $\overline{pp'}$ ,

$$p_h^2 \mathcal{P}(\tilde{k}, \omega) = (2\pi)^{-3} \int d\tilde{\lambda} dt \overline{pp'} e^{i\tilde{k} \cdot \tilde{\lambda} - i\omega t} \quad (7)$$

If the temporal and spatial correlations are assumed to separate in a convecting frame, then a similar separation will occur in the spectra

$$p_h^2 \mathcal{P}_x(\tilde{k}) \mathcal{P}_\tau(\omega) = F \left\{ \tilde{\mathcal{P}}_x(\tilde{\lambda}) \tilde{\mathcal{P}}_\tau(t) \right\} \quad (8)$$

If the pattern is uniformly convected, then the fixed frame spectrum is related to the moving spectrum by

$$p_h^2 \mathcal{P}_x(\tilde{k}) \mathcal{P}_\tau(\omega - k_1 U_c) = F \left\{ \tilde{\mathcal{P}}_x(\lambda_1 - U_c \tau, \lambda_3) \tilde{\mathcal{P}}_\tau(\tau) \right\}, \quad (9)$$

as above.



When the convection is very slow, as on the hull of a ship or on an aircraft at take-off speeds, then  $k_1 U_c \ll \omega$  and the wavenumber and frequency integrations in (6) separate. The resulting power input is equated to the dissipation  $\omega \eta \rho_s \mathcal{U}(\omega)$  and the velocity spectrum given in (2) results. Thus, the infinite plate and finite panel results are consistent at low speeds and we expect them to be at high speeds as well.

The wavenumber pattern for the infinite plate is depicted in Fig. 4. It is similar to Fig. 1 except that now one can relate directly the wave components in the plate with any point on the diagram. Instead of modes, one now has a breakdown into HS, HC, and HF waves. From the analysis, it turns out that the largest response (or power input to the plate) occurs at the intersection of the  $k = k_p$  circle and the HC wave locus. For these waves, the temporal decay of the turbulence is unimportant, its wavenumber spectrum determining the response at  $k = k_p$  and consequently at frequency  $\omega = k_p^2 k c_\ell$ . The formal result is 8/

$$\Pi_{HC} = 4\pi p_h^2 G_\infty \rho_X(k = k_p, \phi_c) / k_p U_c \sin \phi_c, \quad (10)$$

which may be converted to a velocity spectrum by equating input and dissipated power as above. The primary feature of this

result is the absence of  $\mathcal{P}_T(\omega)$ . In simulating the power input from high speed turbulence therefore, one is primarily concerned with simulating a wavenumber spectrum. This spectrum is quite smooth, having roughly a 10 dB variation over 1.5 decades in wavenumber or 3 decades in frequency as seen by reference to Fig. 3.

### III. Response of a supported panel to a sound field

The next step in the simulation is to review our understanding of the absorption of acoustic power by panel structures exposed to a sound field. If the mean square acoustic pressure in a band  $\Delta$  centered about  $\omega$  is  $p_a^2(\omega)$  in the absence of the structure, then the power absorbed by the structure in this band will be <sup>9/</sup>

$$\Pi_a = \frac{2\pi^2 c^2}{\rho_s} \sigma_{\text{rad}} p_a^2 n_s \left\langle D(\Omega) \right\rangle_{\text{inc}} \quad (11)$$

where  $c$  is the sound speed,  $n_s$  is the average modal density of the structure in the band, and  $\sigma_{\text{rad}}$  is the radiation efficiency of the structure. The directivity function  $D(\Omega)$  is averaged over the distribution of energy incident on the panel and the responding modes in the band. For a reverberant field  $\langle D \rangle = 1$  and the absorbed power is uniquely determined by the radiation efficiency.

The radiation efficiency of rectangular supported panels has been computed by Maidanik <sup>10/</sup>. Experimental studies of the radiation of plates with attached stiffening members indicate that these idealized calculations can give quite good estimates of the radiation from structures of engineering interest.

A classification of radiating modes can be made by comparing the wavespeed of their component waves at the resonance frequency with the speed of sound. Modes which have wave components that travel faster than the speed of sound are termed "acoustically fast" (AF). Those with wavespeeds less than the sound speed are called "acoustically slow" (AS). The AF modes occur above the critical frequency in flat panels, but are present below this frequency in curved panels due to the increased stiffness produced by curvature, as Manning and Maidanik have noted.<sup>11/</sup> AS modes may be divided into two groups according to whether or not they have trace velocities along the edge of the structure greater or less than the sound speed. The AS "piston modes" have both trace speeds less than the speed of sound and account for a small part of the radiated sound. The AS "strip modes" have a component of trace speed greater than the sound speed and account for most of the radiation below the critical frequency.

By combining the radiation output of these modal classes it is possible to predict an average radiation efficiency for the panel as Maidanik has done.<sup>12/</sup> A typical form on the result is shown in Fig. 5. An octave or so below the critical frequency  $f_p$ ,  $\sigma_{rad}$  is given by

$$\sigma_{\text{rad}} \simeq \frac{\pi}{\sqrt{3}} \frac{P_r h}{A_p} \frac{c_\ell}{c} \left(\frac{f}{f_p}\right)^{1/2} \quad (12)$$

and it is essentially unity for  $f > f_p$ . In (12),  $P_r$  is the total perimeter of edges and other structural discontinuities on the panel,  $h$  is the panel thickness and  $A_p$  is the panel area.

#### IV. Equivalence between turbulent and acoustic excitation

In the previous sections, we have reviewed the methods and analyses that are available for predicting the average power input into a simple structure in frequency bands. We must now inquire whether we can replace one form of power input with the other, as simulation would require. We must ask this question in two areas; first, what is the difference, if any, in the "direct" vibrational fields and second, what differences are likely to exist in the reverberant vibrational fields of the panels.

The "direct wave" on a panel is like a direct wave in a sound field; it is the free wave that is generated by the disturbance disregarding the additional wave components that are generated when it encounters a structural discontinuity. When the panel is excited by low speed turbulence, the HF waves spread out like waves from a small source of area  $A_t$  and spectrum  $\mathcal{P}_T(\omega)$ . For high speed turbulence on the other hand, the HC waves that are generated travel at an angle  $\phi_c$  from the direction of convection and have a spectrum which does not depend on  $\mathcal{P}_T$  at all but rather on the wavenumber spectrum  $\mathcal{P}_x(k)$ . The energy absorbed from the sound field "enters" the structure at the edges of the panels and the direct wave travels into the panel almost at right angles to

the edge. In this case, one has nearly a line source disturbance. It is clear therefore that the direct field will be quite different in the various cases of turbulent and acoustic loading.

The reverberant field is produced by successive reflections of the energy in the direct wave from the edges of the panel. The power remaining in the direct wave after the first reflection is approximately  $\Pi_0 e^{-kd\eta/4}$  where  $d = \Pi A_p / \rho_a$  is a mean free path for two dimensional systems. The energy in the direct field is approximately

$$E_{\text{direct}} = \frac{\Pi_0 d}{4c_B} \quad (13)$$

while in the reverberant field it is

$$E_{\text{reverberant}} = \frac{\Pi_0}{\omega \eta} \quad , \quad (14)$$

assuming only a very slight energy loss in the first traverse of the wave. Taking the ratio,

$$\frac{E_{\text{reverberant}}}{E_{\text{direct}}} \sim \frac{4}{kd\eta} \quad . \quad (15)$$

For most service structures, the damping is such that  $kd\eta \ll 1$ .

It is therefore more important that the reverberant field be simulated since it contains most of the energy.

The energy in the panel will normally make several passages across the panel before it is dissipated. In addition, there is a passage of energy between panels through the supporting frame. There is a tendency for the idealized modes considered in the theory to be coupled, which may in turn be thought of as a new set of modes having composite properties, with respect to both vibration and radiation, of the old modes. There has not been a great deal of theoretical study of this problem to date, but there is considerable experimental evidence to this effect. For example, reverberant diffuse fields of vibration appear to be set up on laboratory panels when driven either with point shakers (which are very much like low speed turbulence) or with a diffuse sound field.<sup>13/</sup> In addition, there is an experimental reciprocity between the diffuse pressure in a reverberant sound field and the reverberant vibrational field on a structural panel.<sup>14/</sup> This reciprocity basically requires that most of the vibrational modes have comparable coupling to the sound field.

In summary, the vibrational field of structural panels driven by broad band noise appears to be highly reverberant. Because of this, it is somewhat insensitive to the precise



nature of the disturbance and simulation may be possible if the required power levels in the various frequency regions can be supplied by the sound field.

## V. Spectral simulation with a sound field

In this section, we shall review briefly some of the problems associated with predicting the spectral properties of turbulent pressure fields. The central problem, of course, is that the frequency spectrum that one measures with a fixed microphone is not necessarily related directly to the input spectrum of power to the panel. For the HF response to low speed turbulence, the frequency spectrum is set by  $\mathcal{P}_T(\omega)$ , whereas a fixed microphone measures the spectrum

$$\mathcal{P}_M(\omega) = \int_{-\infty}^{\infty} \mathcal{P}_X(k_1 = \omega/U_c, k_3) dk_3 \quad . \quad (16)$$

Information concerning  $\mathcal{P}_T(\omega)$  can be obtained from  $\mathcal{P}_M(\omega)$  by noting from Fig. 3 that  $\mathcal{P}_M(\omega)$  will have a "cut-off" at approximately  $\omega_c = k_1 U_c / \delta_1$ . The characteristic cut-off frequency for  $\mathcal{P}_T$  is  $\theta^{-1}$ , which has been shown by experiment to be approximately  $U_c / 25 \delta_1$ . Thus, the spectrum measured by a fixed microphone is about 25 times as broad as the actual exciting spectrum.

The effect of this indirect relation between loading and response frequencies is illustrated in Fig. 6. When the excitation is acoustic, an increase in level in any band is followed by the same increase (in dB) in the same band of response. If a band level is increased in the fixed microphone response,

this means that a certain group of wavenumbers has been enriched in the spatial wavenumber spectrum. These wavenumbers will cause increased response at lower frequencies in the panel as shown.

In the case of HC modal response to high speed turbulence, the situation is somewhat different. The wavenumbers contributing to the response and microphone pressure respectively are shown in Fig. 7. If one is willing to make a guess at the dependence of the wavenumber spectrum on  $k_3$ , then a measurement of  $\rho_M(\omega = k_1 U_c)$  is sufficient to determine the form of  $\rho_x(\omega = k_1 U_c, k_3)$ . Ffowcs Williams has made such a "guess" and the form he chose was 15/

$$\rho_x(k_1, k_3) = \rho_1(k_1) \cdot \frac{25_1}{\pi(1 + 45_1^2 k_3^2)} \quad (19)$$

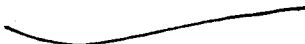
If the angle  $\phi_c$  is less than  $\tan^{-1} [U_c/2\omega_1]$ , then

$$\rho_x(k_1, k_3) \simeq \rho_M(k_1 = \omega/U_c) \cdot \frac{\pi}{25_1} \quad (18)$$

This is not a completely satisfactory way of estimating  $\rho_x(k)$ , but it indicates that the way in which  $\rho_M(\omega)$  is used to infer the spectral character of the input power will be quite different in the high speed and low speed cases.

## VI. Acknowledgement

The author gratefully acknowledges the assistance of many of his colleagues at EBN for many discussions of the problems discussed above. The work received partial support from RTD and NASA.



## REFERENCES

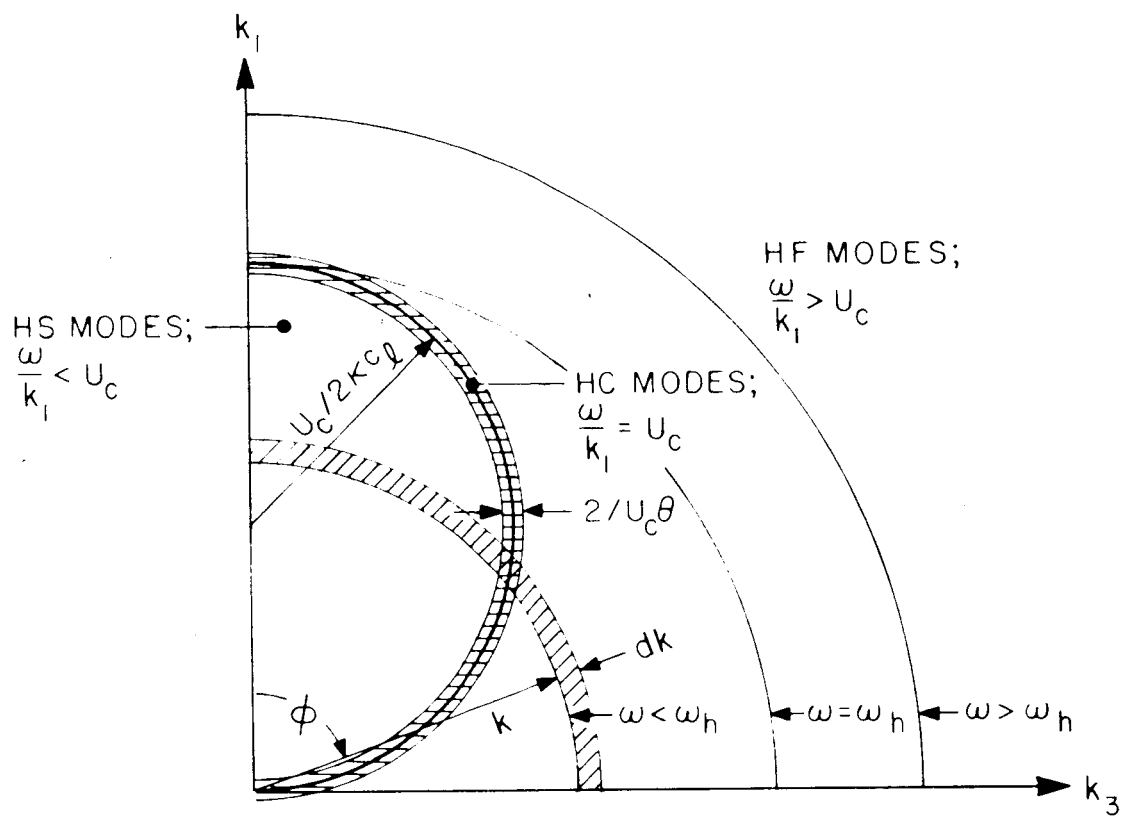
- 1) D. A. Hilton, W. H. Mayes, and H. H. Hubbard, "Noise considerations for manned reentry vehicles," NASA TN D-450, September 1960.
- 2) W. W. Wilmarth and C. E. Wooldridge, "Measurement of the fluctuating pressure at the wall beneath a thick turbulent boundary layer," University of Michigan, Office of Research Administration Report, April 1962.
- 3) G. Maidanik and E. M. Kerwin, Jr., "Acoustic radiation from ribbed plates including fluid loading effects," BBN Report No. 1024, submitted October 1963 to Bureau of Ships.
- 4) I. Dyer, "Sound radiation into a closed space from boundary layer turbulence," BBN Report No. 602, submitted 12 December 1958 to Office of Naval Research, USN. Also, reference 5.
- 5) J. E. Pflowcs Williams and R. H. Lyon, "The sound radiated from turbulent flows near flexible boundaries," BBN Report No. 1054, submitted 15 August 1963 to Office of Naval Research, USN.
- 6) Reference 5, p. 11.
- 7) Reference 5, Fig. 4.

# REFERENCES (Continued)

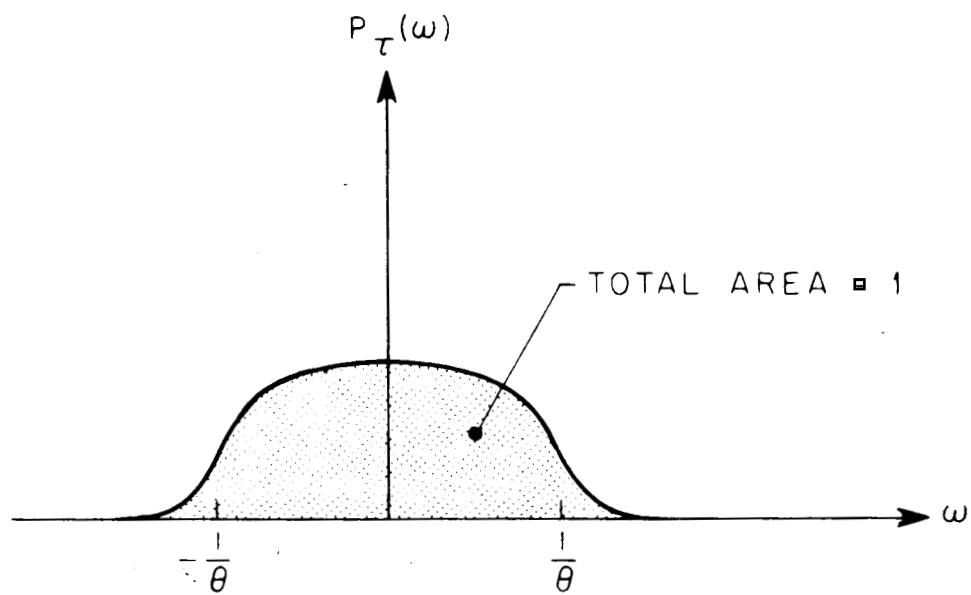
- 8) R. H. Lyon, "Panel excitation by high speed boundary layer turbulence," 67th Meeting of the Acoustical Society of America, 6-9 May 1964, New York, Paper W3. The response of an infinite panel to convected, non-decaying turbulence has been previously computed by H. S. Ribner, "Boundary layer induced noise in the interior of aircraft," UTIA Report No. 37, April 1956.
- 9) R. H. Lyon, G. Maidanik, E. Eichler, and J. Coles, "Studies of random vibration of coupled structures," BBN Report No. 967, submitted 15 November 1962 to Aeronautical Systems Division, USAF, Appendix I.
- 10) G. Maidanik, "Response of ribbed panels to reverberant acoustic fields," J. Acoust. Soc. Am. 34, 6, 809 (1962).
- 11) J. E. Manning and G. Maidanik, "Radiation properties of cylindrical shells," submitted for publication.
- 12) Reference 10, Sec. IID.
- 13) Reference 10, Fig. 11.
- 14) Reference 10, Fig. 14
- 15) Reference 5, p. 12.

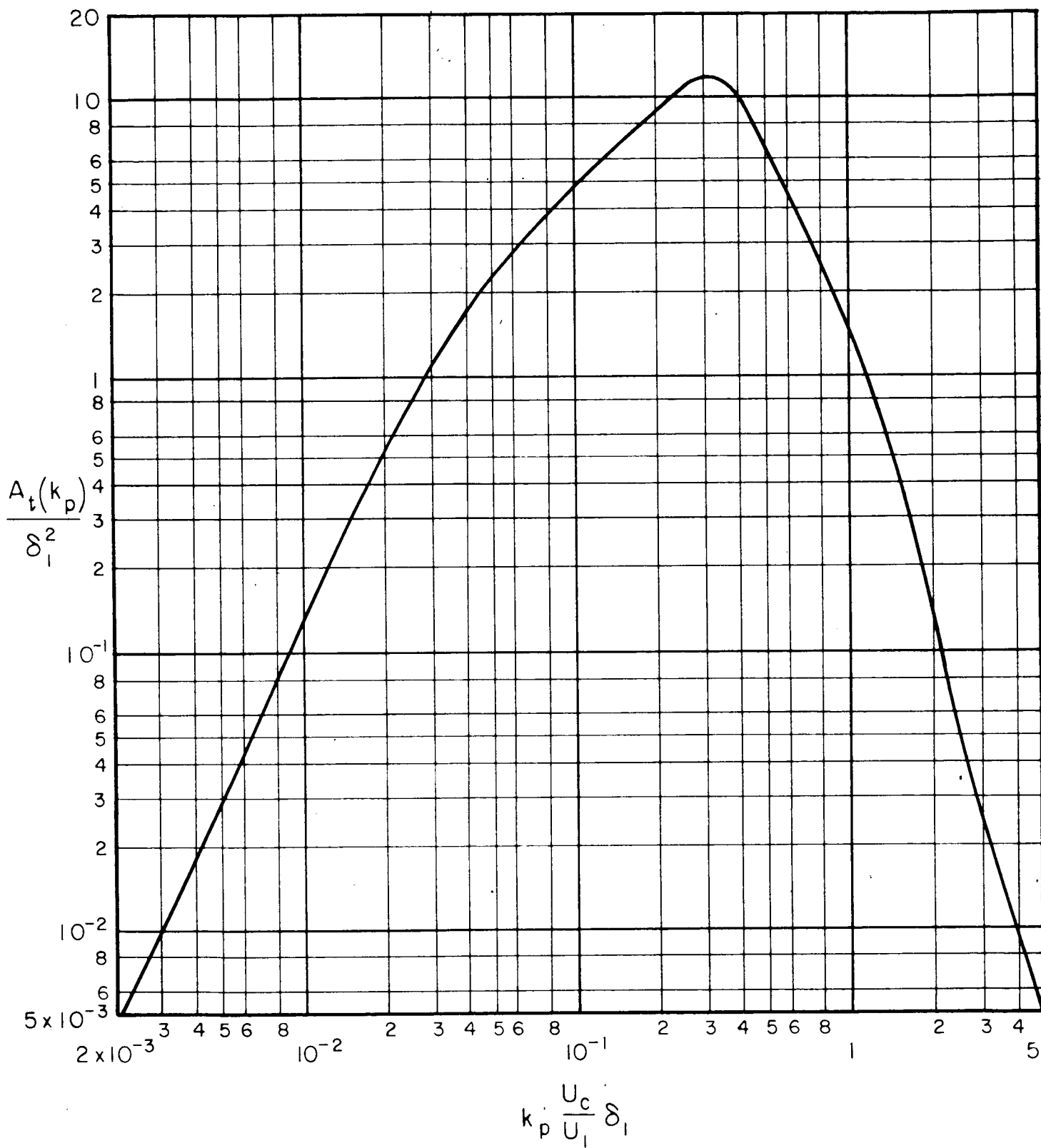
## FIGURE CAPTIONS

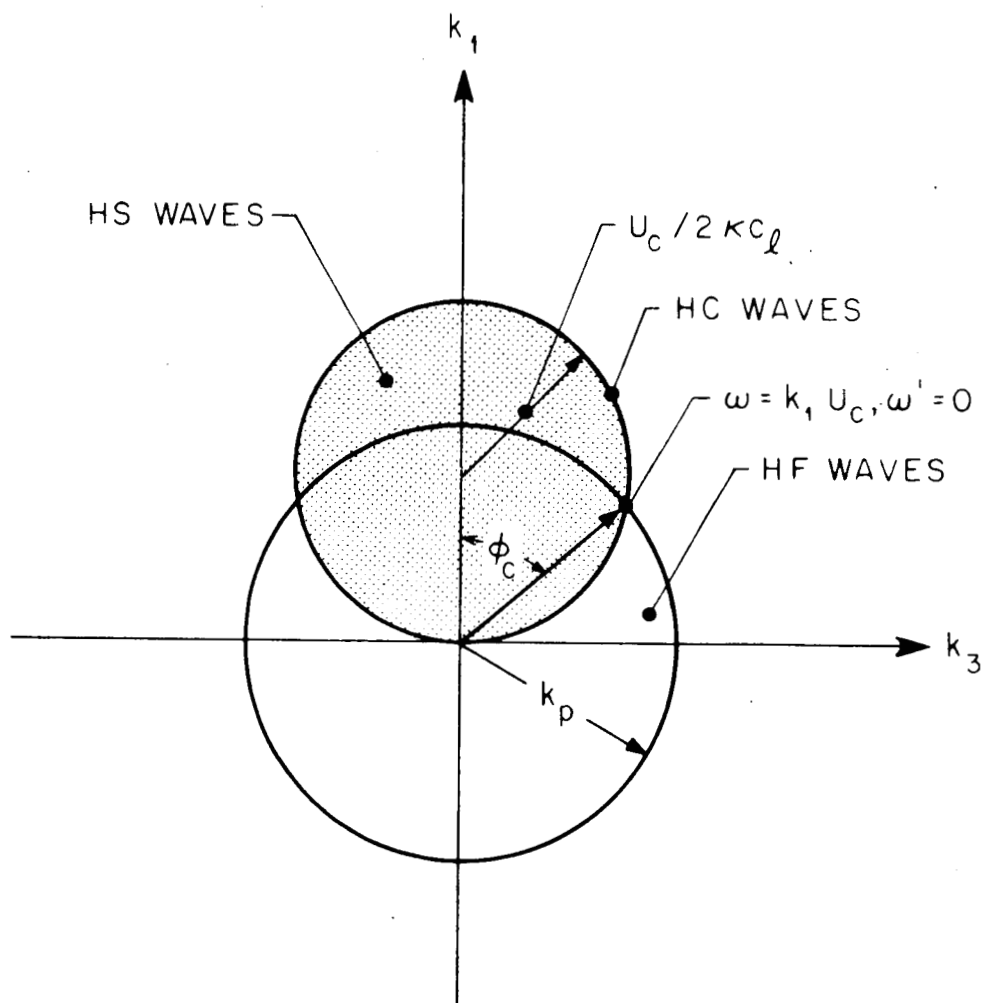
- Figure 1    Plot of wave numbers, pattern in k-space
- Figure 2    Form of the moving axis frequency spectrum
- Figure 3    Effective correlation area for turbulent excitation  
             of HF waves
- Figure 4    HC wave and constant frequency loci in k-space
- Figure 5    Typical radiation efficiency of a supported panel
- Figure 6    Effect of band level changes in measured pressure  
             on response levels in acoustic and low speed  
             boundary layer noise excitations
- Figure 7    Wave numbers producing microphone and panel response  
             in high speed boundary layer noise

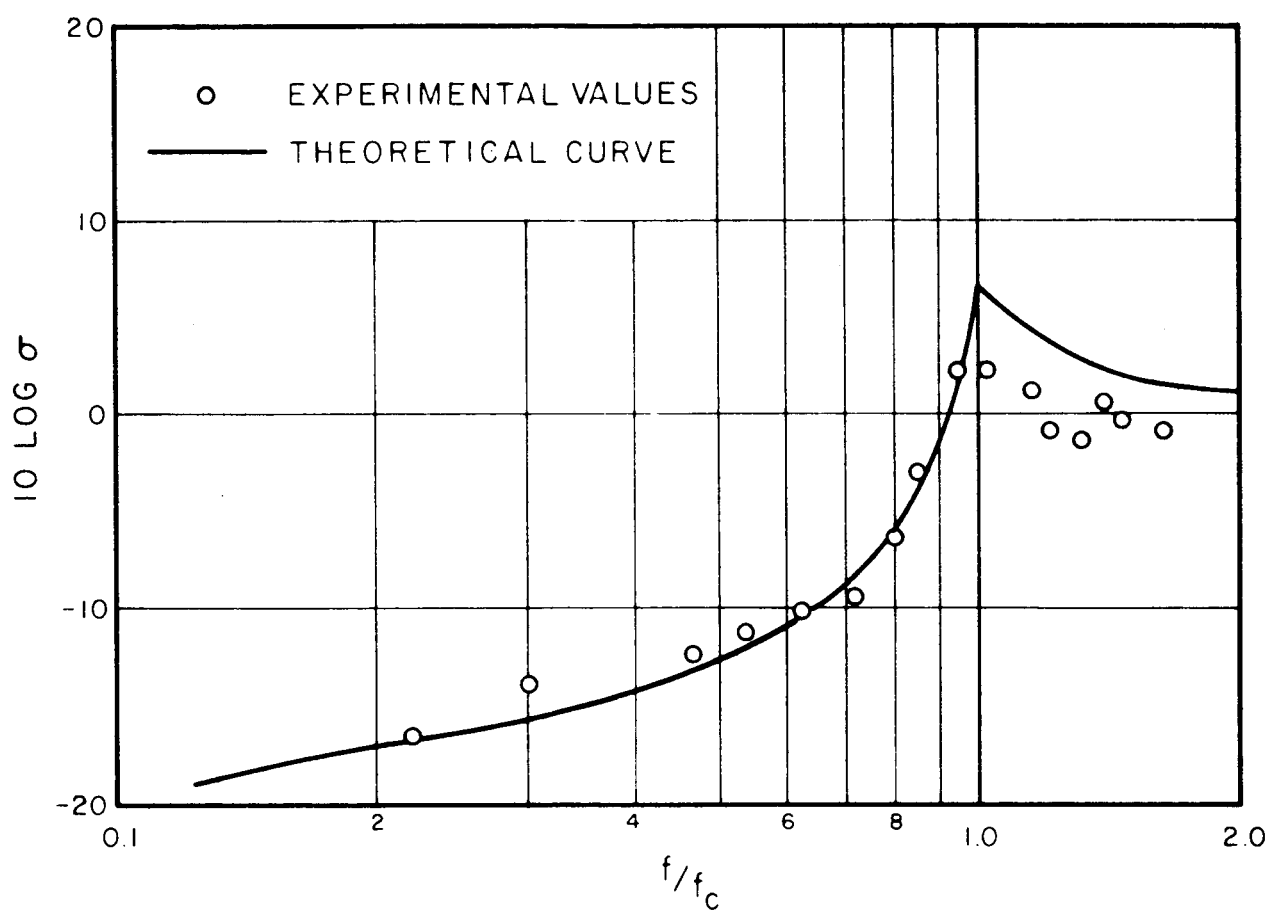


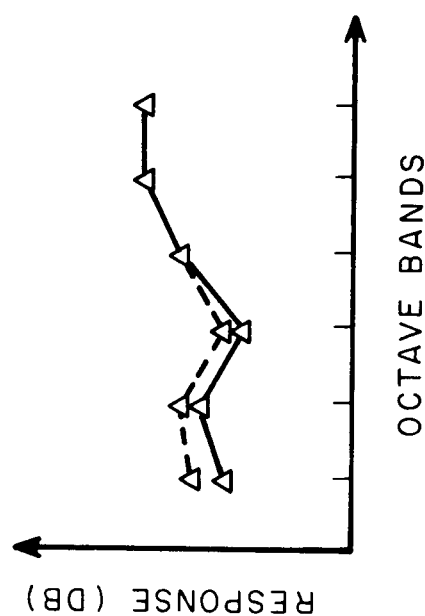
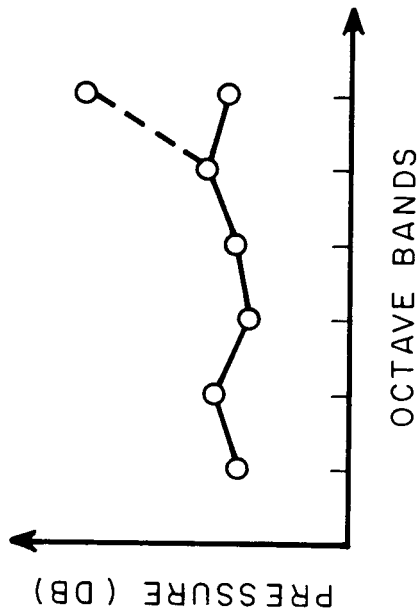




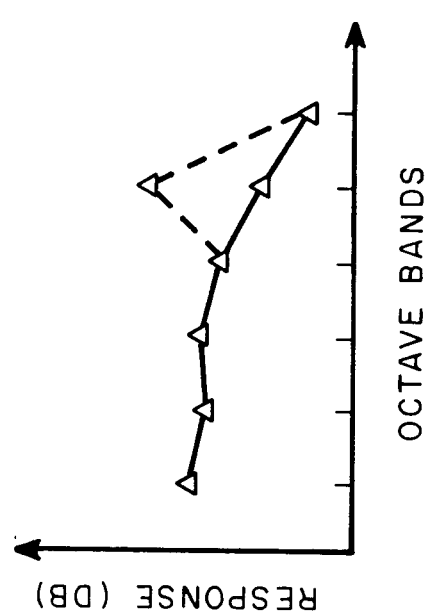
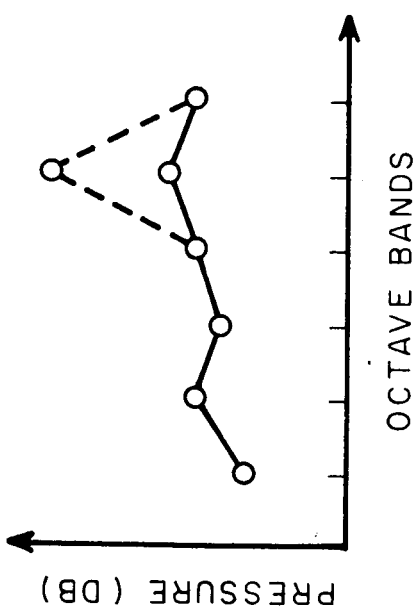








BOUNDARY LAYER EXCITATION



ACOUSTIC EXCITATION

